Lessons learned from E1 Evopod Tidal Energy Converter deployment at Ria Formosa, Portugal

André Pacheco[*], Eduardo Gorbeña[*], Theocharis Plomaritis[*], Jorge Gonçalves[**]

[*] MORE-CIMA, University of Algarve **Centro de Ciências do Mar (CCMAR)

Abstract- This paper presents the results of a pilot experiment with an existing tidal energy converter (TEC), Evopod 1 kW floatable prototype, in a real test case scenario (Faro Channel, Ria Formosa, Portugal). Operational results related to the description of power generation capacity, energy capture area and proportion of energy flux are presented and discussed. The data is now available to the scientific community and to TEC industry developers, enhancing the operational knowledge of TEC technology concerning efficiency, environmental effects, and interactions (i.e. device/environment).

Keywords- Tidal energy; Tidal energy converters; Floatable tidal turbines; Energy production; Ria Formosa, Portugal.

I. INTRODUCTION

The prospects for tidal energy converter technologies very much depend on the specific device concept and how those devices can be optimised to efficiently extract energy, minimizing environmental impacts. The deployment of TECs has been hindered by a lack of understanding of their environmental interactions, both in terms of the device impact on the environment (important for consenting and stakeholder bodies) and environmental impact on the device (fatigue, actual power output, etc.) which is vital to enhance investor confidence and increase financial support from the private sector. The access to freely available, transparently collected monitoring data from real deployments is paramount both for resource assessments and for cataloguing potential impacts of any marine renewable installation.

This paper presents the results from the deployment of a small-scale tidal current turbine (Evopod E1) in a shallow-water estuarine environment, Ria Formosa – Portugal, under SCORE project – Sustainability of using Ria Formosa Currents On Renewable Energy production. This 1:10th scale prototype operated from June to November 2017.

II. STUDY AREA AND PROTOTYPE

The experience with the TEC prototype was performed at Faro-Olhão Inlet, the main inlet of Ria Formosa system (hereafter RF), a coastal lagoon located in the South of Portugal (Figure 1). The RF is a multi-inlet barrier system comprising five islands, two peninsulas separated by six tidal inlets, salt marshes, sand flats and a complex network of tidal channels. The tides in the area are semi-diurnal with typical average astronomical ranges of 2.8 m for spring tides and 1.3 m for neap tides. A maximum tidal range of 3.5 m is reached during equinoctial tides, possibly rising over 3.8 m during storm surges.

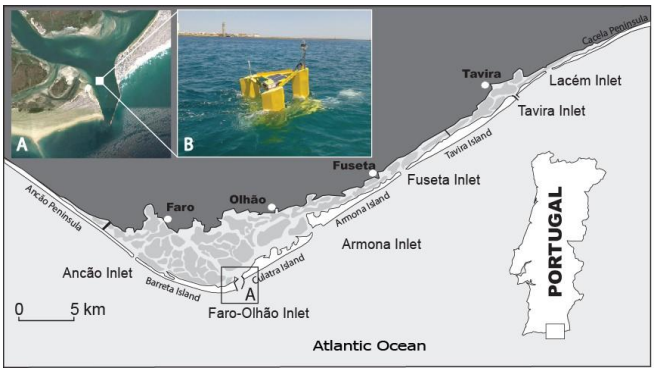

Figure 1 : Deployment site adjacent to Faro-Olhão Inlet (A), the Faro Channel of Ria Formosa lagoon system (Algarve, Portugal), where E1 Evopod (B) operated.

The RF has attracted research interest in all environmental aspects and hence there is a lot of background literature available about biology, morphodynamics and hydrodynamics. The system is particularly adequate for testing floatable TEC prototypes, and representative of the vast majority of transitional systems where TECs can be used to extract energy to power small local communities [1]. Evopod™ is a device for generating electricity from coastal tidal streams, tidal estuaries, rivers and oceanic sites with strong currents (Figure 2). It is a unique floating solution drawing upon proven technologies used in the offshore oil/gas and marine industries [2]. The 1:10th scale Evopod (E1 hereafter) consists of a positively buoyant horizontal cylindrical body of 2 m length and 0.4 m diameter to which are attached three stabilising fins set in a triangle, tethered to a subsurface buoy. Each fin is approximately 1.2 m height, 0.4 m wide and 0.1 thick. A four-bladed 1.5 m diameter turbine made of composite material is attached at the rear of the body and is designed to rotate between 20 and 55 rpm. This result on a maximum blade tip speed of 4.3 ms^{-1}, driving a 1 kW permanent magnet AC generator at a rated flow velocity of 1.7 ms^{-1}. E1 has a cut-in velocity of 0.7 ms^{-1} and it cannot withstand steady flow velocities larger than 1.75 ms^{-1}. The power from the generator feeds a navigation beacon plus an extensive suite of instrumentation measuring

the flow speed, voltage, current, torque, revs, temperature, resistor settings, yaw angle and mooring tension. Data records are logged internally and transmitted to a remote PC through GSM communication.

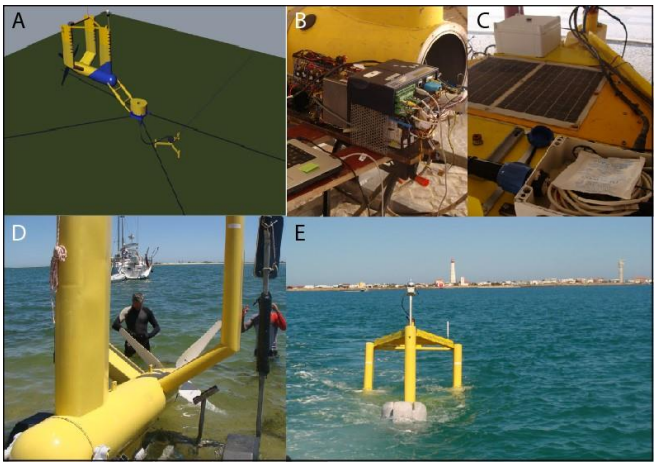

Figure 2 : (A) Scheme of E1 with the mooring lines spreading from the mid-water buoy; (B) inside components connect to the squirrel logger; (C) detail of the deck with the solar panels and control box; (D) E1 launch on the water and (E) it trawl to the deployment site.

III. RESEARCH ELABORATION

The E1 deployment took place on 8th June 2017. The device was tethered to the seabed using a four-line catenary spread mooring system (Figure 3A). The flow speeds, wave and wind characteristics at the deployment site were used for the design of the mooring system. The moorings consists of chain and galvanised wire mooring lines attached to 4 concrete anchors weighting approximately 1 ton each (Figure 3C). The device is a simple fixed pitch downstream turbine, which aligns freely with the predominant current direction.

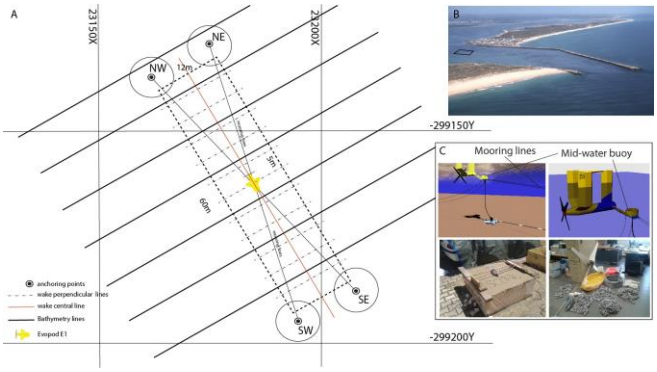

Figure 3 : (A) Scheme of the deployment site, with the mooring locations and line spreading. Also represented are the bathymetry lines 10 m spaced, the wake perpendicular lines and wake central line where bottom-tracking ADCP and static measurements were performed, respectively; (B) Deployment area represented over an oblique image of Faro-Olhão Inlet; (C) mooring scheme and material used on the deployment (e.g. anchoring weight, chains, marking buoys, cable wire, etc).

A load cell was placed for the two south and north lines (Figure 4A), respectively, measuring the tension while E1 is extracting energy. Since the prototype has been deployed for three months, it was not connected to the grid and therefore the excess generated power was dissipated as heat into the sea. The prototype was installed in collaboration with a local marine services company, which was subcontracted to provide a barge boat equipped with a winch (Figure 4B), essential to lower the anchoring weights at their exact planned location, using RTK-DGPS positioning.

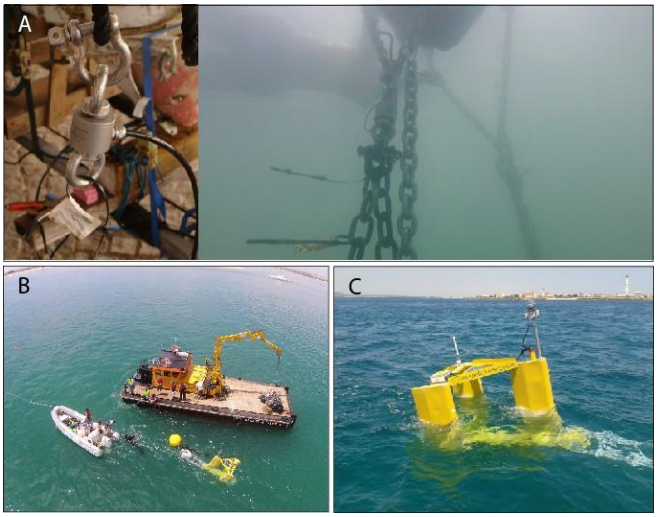

Figure 4 : (A) Detail of the load cells and it placing on the mooring lines; (B) Deployment day and boats used on the mooring operation; (C) E1 deployed on 8th June 2017.

The operation was performed at slack tide and involved a staff of ten people, including skippers, researchers, divers and technical operators, supervised by the maritime authorities. The prototype operated at site (Figure 4C) until the 21st November, when it was towed back to the harbour and removed from the water. All the anchoring system was removed except the anchoring weights that remained on site. Prior to the deployment a baseline marine geophysical, hydrodynamic and ecological database for the pilot site was created. During the operation several datasets were obtained and processed [REF]. Table 1 summarises the data obtained under SCORE project, which are available for download at http://w3.ualg.pt/~ampacheco/Score/database.html.
The E1 is instrumented to continuously monitor and log various parameters. The parameters captured during the RF deployment were: flow speed (ms-1), shaft speed of rotation (RPM), generator output voltage (Volts) and current (Amps), device compass heading (º degree) and mooring tension (kN). The flow speed past the nacelle was measured using an Airmar CS4500 ultrasonic speed sensor. A C100 fluxgate compass from KVH Industries Inc provided compass heading; while mooring tensions, FT, were measured using 0-5kN load cells supplied by Applied Measurements Ltd.

Table 1: SCORE database following the European Marine Energy Centre (EMEC) guidelines

Type of data	Date of Survey	Method used
Bathymetry	2011-2015	LiDAR / Single beam echosounder syncronized with a RTK-DGPS / tide corrected
Side scan sonar	07/2016	Transects performed with a bed imaging system to characterise the bottom of the deployment area in terms of materials and the texture type
Bed characterization	07/2016 – 07/2017	Van Veen dredge operated from the boat.
Habitat characterisation	07/2016 – 07/2017	Bottom trawling, visual census and ROV images to capture, identify and quantify fish species, invertebrates, and epithelial or benthic species on mobile substrate
Tidal currents	03/11/2016 - 17/11/2016	ADP Nortek Signature 1 MHz - bottom mounted on a frame structure, up looking
Tidal currents	03/11/2016 - 17/11/2016	ADP Sontek 1.5kHz Static survey, down looking
Acoustic measurements	19/01/2017 – 14/02/2017	DigitalHyd SR-1
Wake measurements	03/11/2017	ADP Nortek Signature 1 MHz Static E1 centreline profiles at: 5 m up-stream, and 5/10/15/20/25/30 m down-stream.
Wake measurements	03/11/2017	ADP Sontek 1.5kHz Transect survey - E1 transversal profiles 5m spaced within the deployment area. down looking
Turbine performance data	08/06/2017 – 21/11/2017	Evopod E1 data collection

IV. RESULTS & FINDINGS

A bathymetric map of the entire Ria Formosa has been built. The database also provides the mosaic from the side scan survey where main morphological features can be distinguished (i.e. ripples and mega-ripples). An area of about 6 hectares was surveyed using the side scan sonar technique, revealing a seabed mainly composed of sand, coarse sediments and gravel with a high biogenic component.

Species inventory accounted for 31 different species. The epibenthic invertebrate and fish communities were composed of typical and frequent organisms in the soft substrates of Ria Formosa, such as: *Octopus vulgaris, Bugula neritina, Pomatoschistus microps, Holothuria arguinensis, Alicia mirabilis, Sphaerechinus granularis or Trachinus draco*. The use of ROV/video cameras was the most appropriate technique to habitat characterization. A total of 640 images were annotated thoroughly for the presence and quantification of the coverage of the seabed by B. neritina. Percent-cover of this species ranged from 0 to 39.7% (mean: 7.8%) taking into account all images analysed. The image analysis of the seabed showed an increase in the percent-cover of the bryozoan B. neritina during the operation period, from early June to early August. The results on the abundance of B. neritina agree to a moderate extent with the documented natural patterns. Moreover, the increase in the percent-cover of B. neritina was identical in both control and impact areas suggesting that this pattern was not related with the presence of the tidal turbine, but related to environmental factors. Results of the two-month monitoring period showed no evidence of impact on the seabed that could be directly linked to the installation and operation of the turbine.

An acoustic report with estimates of sound pressure levels (SPL) over the entire acquisition period, mainly based on statistical indicators both for broadband SPL and frequency levels, is provided on the database together with time-series of sound pressure levels and frequency, prior to and during the deployment.

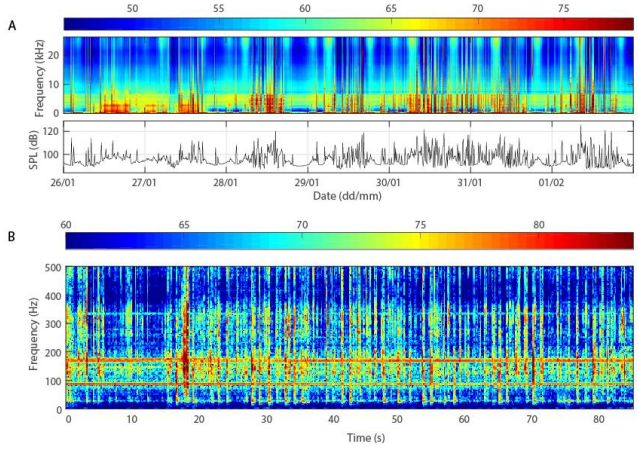

Figure 5 : (A) Time-frequency analysis of the time series collected from 26th January to 1st of February 2017 by means of an autonomous hydrophone mounted on a tripod (only the 2nd half is shown). The analysis has been performed using observation windows of 4096 samples (≈ 0.077 s) which have been averaged to 90 s using the Welch method; (B) Time-frequency analysis data collected at time 15:12 at 8th November 2017 by means of an autonomous hydrophone operated from a boat. The analysis has been performed using observation windows of 16384 samples (≈ 0.311 s).

From a basic frequency analysis over the entire recording time, it was apparent that the site characterized by two distinct periods over 24-hours intervals, where it was evident that periods of reduced boat traffic at night were interchanged with periods of busy boat traffic during the day (Figure 5A). The site of deployment is close to a traffic route leaving or entering the RF system, and therefore idle

and busy regimes were expected a priori to occur. Also, the area of deployment is an area subject to the intensification of water velocities through the fortnight tidal cycle. These two factors are prevailing to the variability observed in the noise level. It is clearly observed that the current speed induced a significant increase on the broadband noise level, especially when current speed peaked to maximum values.

Data collected during E1 operation revealed that the device has minimal potential to generate noise and vibration and therefore does not cause disturbance to the environment. Figure 5B shows a time-frequency representation obtained from the complementary data set recorded on 8th of November 2017, at a position of approximately 5 m upwards from E1, when the current speed was peaking at ~0.56 ms-1. The result indicates that the turbine was radiating at least two frequencies, 86 and 170 Hz, where the higher frequency might be a harmonic of the lower frequency. The 170 Hz frequency shows an outstanding from neighbourhood frequencies of about 10 dB, and the 86 Hz frequency shows an outstanding of 10 to 12 dB. Another harmonic at about 340 Hz appears to be noticed.

Figure 6 shows the vertical profiles of the computed horizontal velocity magnitudes observed for a 14 days interval using the Nortek AS Signature 1 MHz. It is evident the tidal current asymmetry that takes place in the Faro-Olhão Inlet, with ebb currents being significantly stronger than flood currents. These velocity measurements allowed validating the Delft3D model and to select the E1 deployment location [3].

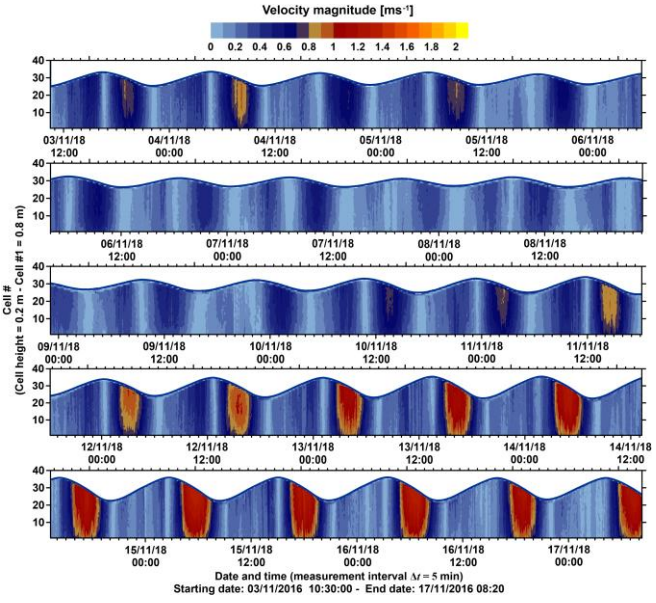

Figure 6 : Time-series of computed horizontal velocity magnitudes at each cell collected with the Nortek AS Signature 1Mz.

The red cross on Figure 7 marks the E1 deployment site which meets the velocity criteria (velocity range between 0.7 and 1.75 ms-1) for around 21% of fortnight cycle. Subsequently, velocity measurements were performed during a spring ebb tide at the deployment location with the ADP Sontek 1.5 kHz, with bottom tracking. Figure 8A shows an example of a time-series contour map of the peak ebb currents at the deployment site, permitting to identify the maximum tidal current velocities that E1 could be exposed; while Figure 8B presents an estimation of the predicted power output. Overall, velocity maximums exceeded the threshold value of ~1.75 ms^{-1} at specific cells, reaching up to ~1.96 ms^{-1}. However, the limit was not surpassed when those cell velocities were averaged by the rotor diameter at time intervals of 5 s, resulting on a maximum averaged flow velocity of ~1.68 ms^{-1}. It can be observed that the rated E1 capacity is almost achieved at peak ebb (~1 kW, Figure 8B), whereas observed power fluctuations are related to turbulence and eddies propagation.

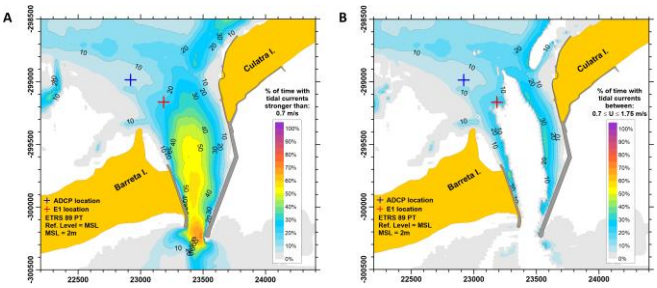

Figure 7 : Percent of time during a 14 period simulation with occurrence of tidal currents for the Faro-Olhão Inlet area : A) with velocities stronger than 0.7 ms-1, and B) with velocities stronger than 0.7 ms^{-1} and lower than 1.75 ms^{-1}.

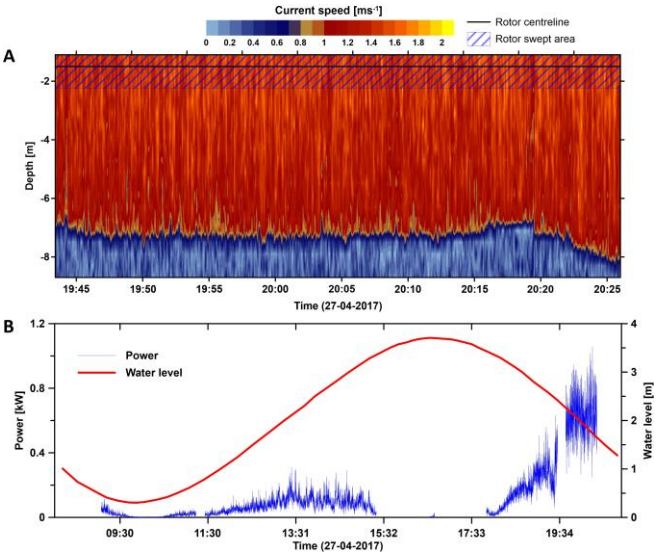

Figure 8 : (A) Peak ebb current velocities measured at E1 deployment site. Each profile corresponds to an ensemble collected with the Sontek ADCP 1.5kHz with bottom tracking at a 5 s interval; (B) estimated electrical power output for E1 based on the ADCP measurements for an ebb spring-tide.

During its operation lifetime, the device had to be pull out of water for maintenance three times due to various failures. Most of the failures occurred with the logging system, which

prevented a continuous data recording and were mainly related to the magnitude of flow velocities during neap tides i.e. there was not enough flow for the turbine to generate and feed voltage to the logger. Figure 9 exemplifies the data recorded by the E1 logger over a spring-neap tidal cycle. From top to bottom the following parameters are presents: (i) drag force recorded by the two load cells; (ii) generated voltage (Volts); (iii) generated amperage (amp); (iv) electrical output (Watts); (v) current speed (ms^{-1}); (vi) raw power (Watts); and (vii) efficiency in power extraction (i.e. electrical outputs divided by raw output).

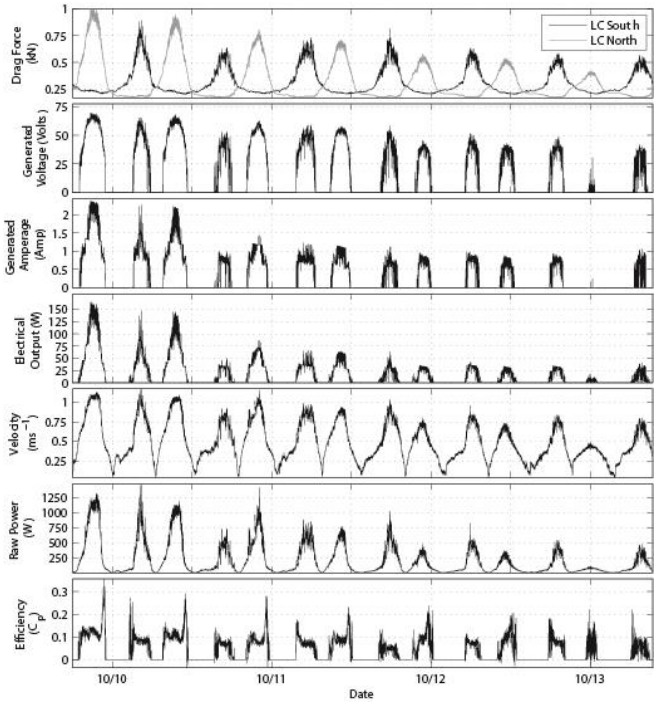

Figure 9 : Time series of E1 parameters during a spring-neap tidal cycle. Fr0m top to bottom the panels present: (i) drag forces recorded by the load cell; (ii) generated voltage; (iii) generated amperage; (iv) electrical output; (v) current speed; (vi) raw power and (vii) E1 efficiency.

In general, and during the peak currents of the spring tides, the shaft speed normally exceed 100 rpm; this values drops to 70 rpm for neap tides. The two load cells values are strongly modulated by the tidal stage. Over spring tides, the drag force can reach to 1 kN. The drag drops to ~0.5 kN during neap tidal ranges. The north mooring under tension during the ebb stage of the flow, which is normally characterized by stronger tidal currents, results in higher load cell values, both in terms of peak values and duration.

Computed thrust coefficients, C_T, are illustrated in Figure 10A. Mean computed values of C_T are 0.44 and 0.4 for load cell South and North, respectively. Larger variation of C_T values are observed for flow speeds below 0.5 ms^{-1}. When flow speed increases, C_T values converge to mean values.

This phenomenon can be explained due to the fact that at higher flow velocities an onset of turbulence in the boundary layer decreases the overall drag of the device. The fitting of a quadratic drag law (Figure 10B) to the measured mooring lines tensions shows that a constant C_T of 0.4 provides a good agreement with the observed flow speeds.

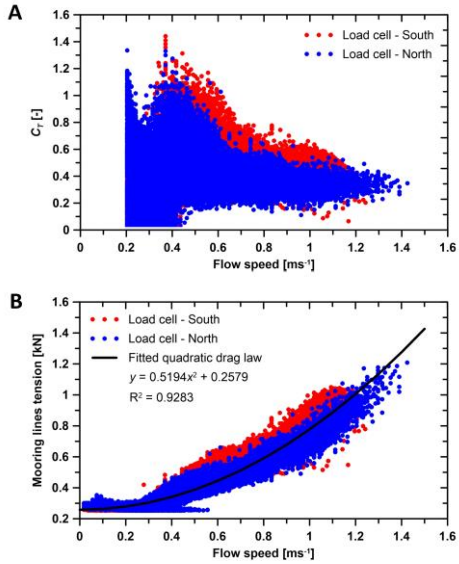

Figure 10 : (A) Computed C_T for both load cells placed at E1 moorings; (B) observed tension forces for both load cells and fitted quadratic drag law.

The electrical parameters voltage and amperage, as well as associated electrical output, are strongly related with more than 100 W produced during spring tidal ranges (Figure 11). This production quickly drops within a couple of days from the larger spring tides. For the rest of the tidal cycles the electrical productions are less than 50 W, or even smaller at the neap cycles.

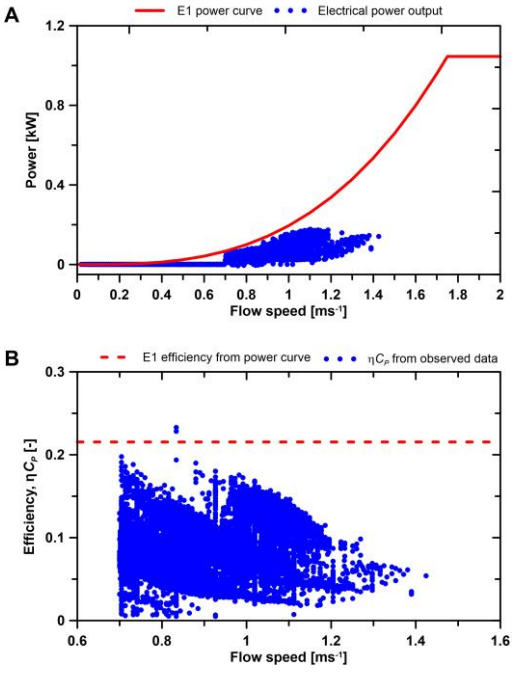

Figure 11 : (A) Comparison between E1' electrical power curve and the observed electrical power outputs; (B) Observed efficiencies, ηC_p, of E1 at various flow speeds.

As expected, the associated tidal currents speed measured from the E1 Doppler sensor are strongly associated with all the above parameters. In fact, and taking as example the electrical output, it is observed that for velocities less than 1 ms^{-1} the produced power drops by a factor of 2. For the same time, the raw power was of the order of 1 kW over the most productive tide phases, dropping to half when the peak tidal currents did not exceed 1 ms^{-1}.

Regarding E1's operating efficiency, the recorded values during the deployment (Figure 9) differ from the power curve provided by the manufacturer and calculated using a constant power coefficient, C_p = 28 %, resulting in a ηC_p = 22 % (Figure 11A) i.e. although the maximum efficiencies observed are of 23 % at 0.8 ms^{-1}, slightly higher than the value of 22 % specified in Equation 1 (i.e. ηC_p), average values are of ~9 %. Overall, efficiencies larger than 15% are observed at flow speeds below 1.1 ms-1 (Figure 11B). Above this flow speed, efficiency starts to drop to an average value of ~6%. For the highest flow speed, 1.42 ms^{-1}, efficiency is ~5.4%. These low efficiency values, and the tendency of efficiencies' decrease with increasing flow speeds, can be related to the load control system of the generator and to flow speed fluctuations. When switching in and out the resistors due to variations on flow speeds causes abrupt oscillations on power output affecting the device' efficiency. It is important to point that the power curve provided by the manufacturer is calculated assuming a constant power coefficient (C_p = 28 %), when usually power coefficients vary with flow speed.

The static wake measurements along E1's wake centreline obtained with the Nortek AS Signature 1 MHz ADCP for a full profile are presented on Figure 12A. Figure 12B summarises the wake velocity deficits for all measured profiles (i.e. U/U_o, relating flow velocities with the presence of the turbine, U, and without turbine U_o) at the rotor horizontal plane' height, for each E1' downstream location (i.e. 5 m, 10 m, 15 m, 20 m, 25 m and 30 m). From Figure 12B, it can be seen how the wake re-energizes gradually downstream E1 and recovers almost completely at a distance of 30 m (i.e. 20 rotor diameters). Immediately behind E1, the wake's vertical distance matches the diameter of the turbine rotor (i.e. 1.5 m).

The distortion of the velocity profile caused by the wake expands progressively at each downstream distance and the minimum flow velocities are found at deeper depths, until the velocity profile recovers it normal shape. This wake recovery pattern is observed in all measured profiles (Figure 12A). From the box plot (Figure 12B), it is observable that the velocity deficits varied from 0.8 (first quartile) at 5 m to 0.97 (third quartile) at 30 m downstream. Median values of velocity deficits increase with distance as wake recovers. At closer distances downstream E1, it is sensed a larger deviation of velocity deficits. This can be related to the fact that, in the near wake, velocity gradients are larger and its width is shorter than in the far wake. Thus, at these locations, small changes in the lateral position of the ADCP produce larger variabilities on the measured velocities.

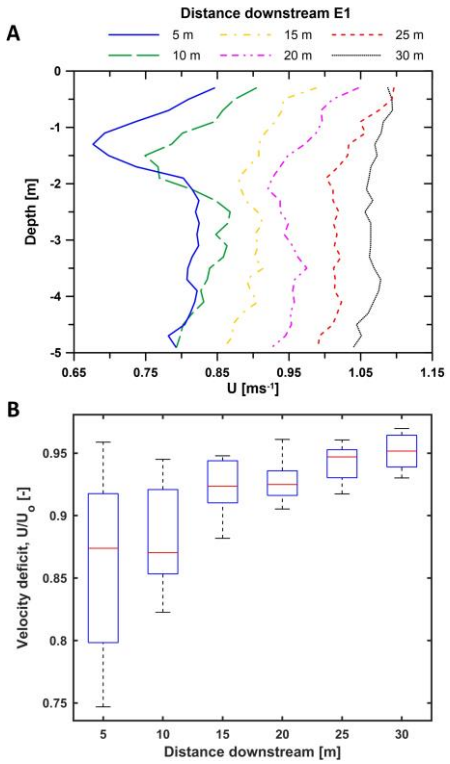

Figure 12 : (A) Example of the static wake profiles measured with the Nortek AS Signature 1 MHz at different E1' downstream distances; (B) Box plot of wake centreline velocity deficits (U/Uo) at E1' rotor height.

V. CONCLUSION

The innovative aspect of E1 testing in Portugal laid with the unique morphological characteristics associated with the device deployment site at RF, a coastal lagoon protected by a multi-inlet barrier system. Some key lessons were highlighted [4]:

(1) No collisions or major interactions occurred with wildlife and mooring weight were rapidly colonized by the typical species normally present in the area;

(2) The high energy environment coupled in a restricted work area, heavy chain moorings and a tidal turbine with rotating blades made the use of traditional biological sampling techniques a challenging task. Among the methods tested, the video sledge proved to be the most reliable to be used in these demanding environmental conditions;

(3) The results from the assessment of the soft sediment community in the study area during the monitoring period did not show signs of disturbance that could be directly linked with the presence of neither the turbine nor the mooring system used;

(4) The amount of acoustic energy introduced into the aquatic environment is limited in frequency band and time. Yet, further analysis is required to conclude on the acoustic impact in the surrounding area and how it would extrapolate

if an array of floatable TECs in real-scale were to be deployed;
(5) Overall, the physical environmental impact from E1 small-scale TEC pilot project was found to be reversible on decommissioning, especially because the chosen area is characterized by a high current flow that already causes natural disturbances to the bed. No record of any change on the bed related with alteration of either flow or sediment transport patterns;
(6) The exact calculation of mooring loads using safety factors was essential to the success of the deployment. However, the miscalculation of the exact location of one of the mooring weights caused over tension on one of the mooring lines, which interfered with the reposition of the device when turning until the tension was corrected by lengthening the mooring line;
(7) The flow field around turbines is extremely complex. Variables such as inflow velocity, turbulence intensity, rotor thrust, support structure and the proximity of the bed and free surface all influence the flow profile. A full characterisation of the 3D flow patterns was performed using ADCPs (moored and boat-mounted surveys). The data collected allowed validating a numerical modelling platform, essential to accurate positioning the device based on the environment/device constraints, mainly in which concerns cut-in/cut-off velocities and deployment depth. The static measurements performed during device operation were effective on characterizing the wake at different distances from the device and represent a valid data set for wake modelling validation;
(8) E1 proved to be easy to disconnect from the moorings and it transport inshore for maintenance and repair was relatively straightforward. This is an important aspect, since installation/maintenance costs represent a major drawback of TEC technologies for future investors;
(9) Biofouling can be a major issue affecting performance of devices operating in highly productive ecological regions like RF. Therefore, maintenance operations need to be planned in advance to control the lifespan of antifouling coatings, especially on the leading edge of blades;
(10) Model data is essential for future planning and testing floating TEC prototypes on other locations by providing values of turbine drag, power coefficients and power outputs for different flow conditions and operating settings [27]. Mooring loads and flow speeds data allowed to calculate time-series of E1 drag coefficient. By fitting a quadratic drag law a constant drag coefficient of 0.4 was obtained for flow speeds up to 1.4 ms-1. In order to confirm this estimation it will be necessary to measure mooring tension loads at higher flow speeds;
(11) The operational data collected during the operational stage allowed the monitoring of device performance and serve as basis for developing advanced power control algorithms to optimise energy extraction under turbulent flows. The measured energy extraction efficiency and mooring loads of the operational prototype can now be compared against numerical models in order to validate these tools. Time series of measured efficiency revealed an overall underperformance of E1 respect to its power curve estimations with values of ηC_P below 20% most of the time. Further research has to be conducted to accurately identify the causes of low efficiencies and determine if the problem is related with mechanical, electrical and/or generator losses. A preliminary diagnose points to the generator's resistors control strategy, which needs to be optimised to increase electrical power outputs when operating in turbulent flows;
(12) Efficiency data obtained with E1 prototype can be scale up for proposing realistic tidal array configurations for floating tidal turbines and on supporting the modelling of mooring and power export cabling systems for these arrays.

ACKNOWLEDGMENT

The paper is a contribution to the SCORE project, funded by the Portuguese Foundation for Science and Technology (PTDC/AAG-TEC/1710/2014). André Pacheco was supported by the Portuguese Foundation for Science and Technology (IF/00286/2014/CP1234). Eduardo G-Gorbeña has received funding from the Marie Skłodowska-Curie Actions of the European Union's H2020-MSCA-IF-EF-RI-2016 / under REA grant agreement n° [748747].

REFERENCES

[1] Pacheco A, Ferreira Ó, Carballo R, Iglesias G. (2014). Evaluation of the tidal stream energy production at an inlet channel coupling field data and modelling. Energy 71: 104-117.
[2] Mackie, G. (2008). Development of Evopod tidal stream turbine. In Proc. Int. Conference on Marine Renewable Energy. The Royal Institute of Naval Architects, London, pp. 9–17.G.
[3] Gorbeña, E., Pacheco, A., Plomaritis, T., Sequeira, C. (2017). Assessing the Effects of Tidal Energy Converter Arrays on Hydrodynamics of Ria Formosa (Portugal). 12th European Wave and Tidal Energy Conference, Cork, Ireland, 27/08 - 01/09.
[4] Pacheco, A., Ferreira, Ó. (2016). Hydrodynamic changes imposed by tidal energy converters on extracting energy on a real case scenario. Applied Energy 180: 369-385.
[5] Pacheco, A., Gorbeña, E., Plomaritis, T.A., Garel, E., Gonçalves, J.M.S., Bentes, L., Monteiro, P., Afonso, C.M.L., Oliveira, F., Soares, C., Zabel, F.3, Sequeira, C. (under review). Deployment characterization of a floatable tidal energy converter on a tidal channel, Ria Formosa, Portugal.

AUTHORS

First Author – André Pacheco, PhD, CIMA-UALG, ampacheco@ualg.pt.
Second Author – Eduardo Gorbeña, PhD, CIMA-UALG, egeisenmann@ualg.pt.
Third Author – Theocharis Plomaritis, PhD, CIMA-UALG, tplomaritis@ualg.pt.

Forth Author – Jorge Gonçalves, PhD, CCMAR, jgoncal@ualg.pt.

Correspondence Author – André Pacheco, ampacheco@ualg.pt.